RAPID COMMUNICATIONS

PHYSICAL REVIEW C VOLUME 52, NUMBER 3 SEPTEMBER 1995

$(d, {}^2\mathrm{He})$ reactions at $E_d = 125.2$ MeV

H.M. Xu, G.K. Ajupova, A.C. Betker,* C.A. Gagliardi, B. Kokenge, Y.-W. Lui, and A.F. Zaruba
Cyclotron Institute, Texas A&M University, College Station, Texas 77843
(Received 5 May 1995)

We have measured cross sections for $(d, {}^2\mathrm{He})$ induced reactions on the p-shell nuclei ^{6}Li, ^{12}C, and ^{13}C and the sd-shell nucleus ^{24}Mg at an energy of $E_d = 125.2$ MeV. The measured excitation energy spectra are very similar to those from (p,n), (n,p), and $(d, {}^2\mathrm{He})$ reactions at higher energies. The measured $0°$ $(d, {}^2\mathrm{He})$ cross sections show a remarkably well-defined linear relation with the Gamow-Teller strengths deduced either from β decay or from (p,n) reactions. Our results demonstrate that the $(d, {}^2\mathrm{He})$ reaction can be used as a powerful tool to study Gamow-Teller strengths in the β^+ direction at energies as low as $E_d = 125.2$ MeV.

PACS number(s): 25.45.Kk, 25.40.Kv, 27.20.+n, 27.30.+t

Charge-exchange reactions at intermediate energies have proven to be a powerful probe of nuclear structure and reaction dynamics, particularly spin-isospin excitations [1–3]. Extensive studies have been performed on (p,n) reactions at the IUCF, TRIUMF, and LAMPF [1,3–6]. These studies indicate that the observed Gamow-Teller (GT) strengths are consistently below the GT sum rule [7], constituting the so-called *missing* GT strength. Even for well-isolated states, the observed strengths are often more than 40% [3] below those predicted by the most accurate shell model calculations available [8–11], constituting the so-called *quenched* GT strength. To explain these apparent missing or quenched strengths, various mechanisms—including ground-state random phase correlations [3,8,9,11], subnucleonic degrees of freedom [12], or mistreating of real GT strengths as "experimental background" [3,11]—have been proposed.

The (p,n) reactions only probe GT strength distributions in the β^- direction, which represents decreasing T_z for a target with a neutron excess. To compare rigorously with the GT sum rule, one also needs to measure the corresponding GT strengths in the β^+ direction. Besides complementing the β^- reactions, GT strengths in β^+ reactions play a unique role in understanding β capture and nucleosynthesis in supernova processes [13] and the size of matrix elements in double-β decay processes [14]. It is possible, in principle, to infer GT strengths in the β^+ direction from the populations of the analogs of the states of interest in a (p,n) reaction study. However, reactions that probe β^+ GT strength directly have several appealing features. (1) For a target with a neutron excess and ground-state isospin T_0, β^+ reactions excite a unique isospin T_0+1. Furthermore, these final states represent the low-lying states of the final nucleus. In contrast, β^- reactions on such a target excite states of isospin, T_0-1, T_0, and T_0+1. The T_0+1 states, which are the analogs of the states populated in a β^+ reaction, are frequently obscured by states of lower isospin, especially if they are only populated weakly. (2) The isospin geometric factors strongly favor the excitation of T_0+1 states in β^+ reactions compared to β^- reactions: e.g., $B(\mathrm{GT})_{\beta^+}/B(\mathrm{GT})_{\beta^-} = (T_0+1)(2T_0+1)$, for reactions on the same target populating analog final states. (3) For light and medium-mass nuclei with small neutron excesses, the three-body breakup thresholds for β^+ reactions come at much higher excitation energies in the residual nucleus than those for β^- reactions. Indeed, intermediate energy (n,p) reactions have been carried out experimentally for several nuclei [15–19]. However, the data are still scarce mainly because neutron beams can only be produced as a secondary beam, so the counting rates are usually low. As a result, the energy resolution is often poor, usually 1 MeV or worse. This poor resolution can sometimes make interpretation of the data difficult [14]. Heavy-ion charge-exchange reactions such as $(^{12}\mathrm{C}, {}^{12}\mathrm{N})$ have also been used in measuring β^+ strengths [20,21]. For such reactions, however, the reaction mechanisms are complicated and successive transfer reactions could dominate at energies below $E/A \approx 100$ MeV [20–22].

Intermediate energy $(d, {}^2\mathrm{He})$ reactions can be used as an alternative tool to measure β^+ strengths. Since the deuteron and ^{2}He are the simplest complex particles, the reaction mechanisms are expected to be much simpler than those using heavier beams such as $(^{12}\mathrm{C}, {}^{12}\mathrm{N})$. Moreover, the one-step reaction mechanism for $(d, {}^2\mathrm{He})$ is expected to occur at substantially lower energies. Though the reaction mechanisms are more complicated than those for (n,p) reactions, $(d, {}^2\mathrm{He})$ reactions have at least two significant advantages. The reactions can be performed with primary beam, rather than the secondary beam in (n,p) reactions. Thus, experiments can be performed with high counting rates and improved energy resolution. Meanwhile, for one-step reactions the $1^+ \rightarrow 0^+$ quantum numbers in $(d, {}^2\mathrm{He})$ ensure a spin-flip transition. Hence, the reactions can be readily used to study the Gamow-Teller ($\Delta S=1$, $\Delta L=0$, $\Delta T=1$) or spin-flip dipole ($\Delta S=1$, $\Delta L=1$, $\Delta T=1$) strength distributions. In contrast, (n,p) reactions need a secondary scattering to determine the spin transfer unambiguously. The $(d, {}^2\mathrm{He})$ reaction, however, has two major disadvantages. Foremost, the reaction mechanism is not well understood at present. In addition, one has to detect the two correlated protons from the $^1S_0$ state of ^{2}He, which are emitted in nearly the same direction, in the presence of a large proton background resulting from deuteron breakup reactions. This could be particularly troublesome at zero degrees where deuteron breakup cross sections are much larger than the Gamow-Teller cross

*Present address: Cyclotron Facility, Indiana University, Bloomington, Indiana 47408.

sections of interest. Thus, special detection systems are required to study $(d,{}^2\mathrm{He})$ reactions.

$(d,{}^2\mathrm{He})$ reactions were first investigated at beam energies of $E_d = 55$ to 99 MeV [23–26]. At forward angles, the observed cross sections were consistent with a direct, one-step charge-exchange mechanism. However, the measured angular distributions were not characteristic of particular angular momentum transfers. In particular, the $\Delta L=0$ transitions were neither noticeably enhanced in magnitude nor easily identifiable by virtue of their shape. It was thus concluded that the $(d,{}^2\mathrm{He})$ reactions cannot provide useful information concerning $\Delta L=0$, $\Delta S=1$, $\Delta T=1$ strength distributions at energies $E_d \leq 99$ MeV. These earlier studies, however, were performed with detector telescopes and cross sections were only measured at angles $\theta > 10°$. In contrast, a recent spectrograph study at RIKEN [27,28] shows a well-defined linear relation of $(d,{}^2\mathrm{He})$ zero-degree cross sections with known GT strengths from β decays at $E_d=260$ MeV, indicating the usefulness of $(d,{}^2\mathrm{He})$ in studying GT strengths. At much higher beam energies, 650 MeV and above, a one-step spin-flip process was observed in the Δ resonance regime [12]. The latter, however, provides little information concerning the strength distribution in the low lying states.

The purpose of this Rapid Communication is to demonstrate that there exists a well-defined proportionality between the $(d,{}^2\mathrm{He})$ zero-degree cross sections and known Gamow-Teller strengths at energies as low as $E_d=125.2$ MeV. The existence of such a relation will not only put our understanding of the $(d,{}^2\mathrm{He})$ reaction mechanism on a surer quantitative footing; it will also provide us with a calibration and allow us to study β^+ GT strengths inaccessible to β decay, which are important in supernova and double-beta-decay processes.

The experiment was performed using 125.2 MeV deuteron beams from the Texas A&M University K500 superconducting cyclotron. Several self-supporting targets, including CH_2 (7 mg/cm^2), ^{6}Li (26 mg/cm^2), C (10 mg/cm^2), ^{13}C (14.8 mg/cm^2), and ^{24}Mg (1.95 mg/cm^2), were used for the present study. An optimized detection system, the Texas A&M Proton Spectrometer [29], was used to detect the correlated protons from ^{2}He decay. The proton spectrometer includes a magnetic spectrometer with point-to-parallel optics, two drift chambers, and X and Y scintillator trigger arrays. Each of the two drift chambers consists of five sense wire layers—two x-layers, one diagonal layer, and two y layers. To minimize multiple scattering, a gas mixture of 20% Ne and 80% C_2H_6 is used for the drift chambers [30]. Charged particles are traced through the two drift chambers. Their energies and scattering angles are then determined using the results of a detailed field map of the magnet. The solid angle for detecting an individual proton is nearly 20 msr, while the effective solid angle for detecting a ^{2}He within a fiducial region ($\Delta\theta \leq 3°$, $\Delta\phi \leq 1°$) is ≈ 1.5 msr. The acceptance in θ is flat over the fiducial region. A beam stop mechanism, consisting of several Faraday cups, stops the beam inside the spectrometer magnet at small scattering angles ($\theta \leq 7°$), near the entrance to the magnet at intermediate scattering angles, and outside the magnet in the target chamber at large scattering angles ($\theta \geq 15°$). Two different triggers are used to take data. A singles trigger requires at least one hit in each of the two scintillator arrays. At large scattering angles, it provides a virtually pure sample of individual proton tracks that can be used to calibrate the drift chambers. At all angles, it may be used to investigate the sources of background protons that lead to random coincidences. The ^{2}He trigger requires at least one hit in one of the two scintillator arrays, together with a nonadjacent pair of hits in the other array. This trigger is satisfied by p-p coincident events, both from actual ^{2}He decays and from accidental coincidences, and by random p-n and p-d coincidences.

Calibration of the detection system was performed off-line using the observed cross over angles between $^1\mathrm{H}(d,{}^2\mathrm{He})n$ and deuteron-induced reactions on the heavier targets, notably ^{6}Li and ^{12}C, and the independence of the measured reaction Q value on the ^{2}He scattering angle, θ_{in}, for each target. The measured Q value depends on the reconstructed energy and angle of the ^{2}He, which, in turn, depend on the magnetic matrix elements and detector positions. The measured Q vs θ_{in} relation provides a powerful constraint on these parameters. Moreover, data from different targets, which have different Q values and different masses, and therefore, different recoil effects, provide checks over a wide range of the acceptance of the proton spectrometer. Using the above two criteria, we were able to determine the incident beam angle to better than 0.1° and the beam energy to better than 200 keV (which is more accurate than that provided by the cyclotron tune parameters). The ^{2}He energy resolution for the present study was 600–700 keV full width at half maximum (FWHM). The ^{2}He angular resolution was better than 0.4° FWHM. The p-n and p-d events were eliminated off-line using cuts on the pulse height in the scintillators and multiplicities in the drift chambers, as well as cuts on the reconstructed tracks themselves. Random p-p coincidence events in which one or both of the protons originated in the beam stop were eliminated by requiring both tracks to point back to the target. The detailed performance of our detection system will be described in a forthcoming publication.

As an example, Fig. 1 shows the excitation functions of $^{12}\mathrm{C}(d,{}^2\mathrm{He})^{12}\mathrm{B}$ reactions measured at 0°, 5°, 10°, and 15°, respectively, after subtracting the random coincidence backgrounds obtained from two protons triggering in neighboring beam bursts. The spectra are shown as a function of E^*, the excitation energy in ^{12}B after correcting for the reaction Q value. Essentially, no events are recorded at excitation energies $E^* < 0$ after subtracting the random backgrounds, indicating the backgrounds were well understood. (The backgrounds are typically a few counts per bin or less for Fig. 1. We have taken data on other targets with much higher random backgrounds, and the subtractions are equally good.) To ensure that the two protons are from the $^1S_0$ state of ^{2}He, an off-line cut on the relative energy of ^{2}He, $E_{\mathrm{rel}} \leq 1$ MeV, has been used. Although the data were measured at much smaller angles, where the proton background due to deuteron breakup is high, the spectra are much cleaner than those obtained from detector telescopes [23–26]. The strongest peak at $E^* \approx 0$ MeV, which decreases at larger angles, indicates the dominant $\Delta L=0$ transition to the 1^+ ground state of ^{12}B. The shoulder at $E^*=0.96$ MeV reflects the transition to the 2^+ first excited state of ^{12}B. The second peak at $E^* \approx 4.4$ MeV whose magnitude increases relative to

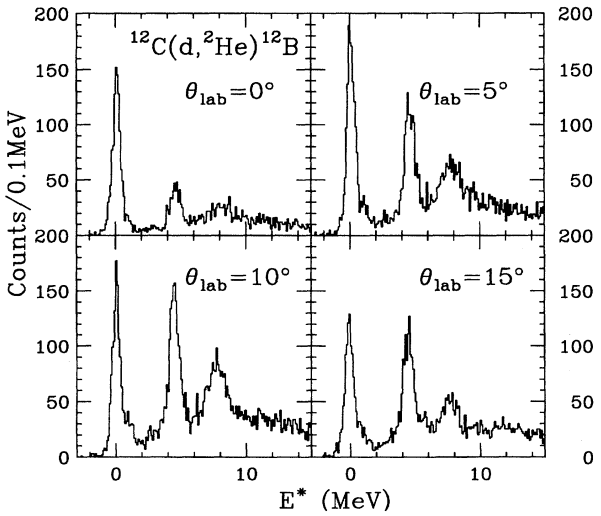

FIG. 1. The measured spectra for ^{12}C(d,^{2}He)^{12}B reactions at 0° (upper left), 5° (upper right), 10° (lower left) and 15° (lower right) at E_d=125.2 MeV as a function of the excitation energy E^* of the residual ^{12}B.

the ground state at larger scattering angles, and the broad third peak at $E^*\approx$ 7.7 MeV represent transitions to spin-dipole and other negative-parity states seen also in (p,n), (n,p), and (d,^{2}He) reactions at much higher energies [2,15,17,27]. Overall, the spectra are very similar to those obtained at higher energies, indicating the usefulness of the (d,^{2}He) technique at K500 cyclotron energies.

The three panels of Fig. 2 show the 0° spectra for the other targets—^{6}Li, ^{13}C, and ^{24}Mg, respectively. The peak in Fig. 2(a) at $E^*\approx$ 0 corresponds to the Gamow-Teller transition from the 1^+, T=0, ground state of ^{6}Li to the 0^+,

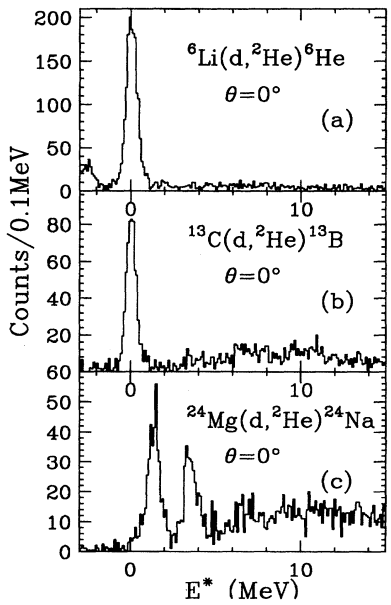

FIG. 2. Same as Fig. 1, but for deuteron-induced reactions at 0° on ^{6}Li (top), ^{13}C (middle), and ^{24}Mg (bottom).

TABLE I. Summary of the results.

Target (J^π)	Residual (J^π,E*) (MeV)	logft	B(GT)	$d\sigma/d\Omega$ (mb/sr)
^{6}Li(1^+)	^{6}He(0^+,g.s.)	2.91	1.62 [a]	2.12±0.07
^{12}C(0^+)	^{12}B(1^+,g.s.)	4.07	1.01 [a]	1.25±0.06
^{13}C($\frac{1}{2}^-$)	^{13}B($\frac{3}{2}^-$,g.s.)	4.01	0.77 [a]	1.00±0.05
^{24}Mg(0^+)	^{24}Na(1^+,0.47)	5.80	0.018 [a]	0.08±0.04
	^{24}Na(1^+,0.47)		0.05 [b]	0.08±0.04
	^{24}Na(1^+,1.35)		0.61 [b]	0.84±0.06
	^{24}Na(1^+,3.41 and 3.59)		0.42 [b]	0.52±0.05

[a]Deduced from the β decay logft value. The logft values are taken from Ref. [31].
[b]Deduced from (p,n) reactions, Ref. [6].

T=1, ground state of ^{6}He. The broad peak at $E^*\lesssim -2$ MeV corresponds to ^{1}H(d,^{2}He)n transitions due to hydrogen contamination in the target. The peak in Fig. 2(b) corresponds to the Gamow-Teller transition from the $\frac{1}{2}^-$, $T=\frac{1}{2}$, ground state of ^{13}C to the $\frac{3}{2}^-$, $T=\frac{3}{2}$, ground state of ^{13}B. These strong transitions, which peaked at $E^*\approx$ 0 MeV in Figs. 1 and 2(a) and 2(b), all have analogous transitions in β decay [31]. Their well-studied logft values, including the corresponding Gamow-Teller strengths after correcting for the spin geometric factors for (d,^{2}He), are listed in Table I.

Figure 2(c) shows the 0° spectrum for the ^{24}Mg(d,^{2}He)^{24}Na reaction. The overall profile is very similar to corresponding studies in (p,n) [6] and (d,^{2}He) [28] reactions at higher energies. The two strong peaks in Fig. 2(c) correspond to transitions from the 0^+, T=0 ground state of ^{24}Mg to four 1^+, T=1 states in ^{24}Na—a weak peak at 0.47 MeV, a strong peak at 1.35 MeV, and two peaks at 3.41 and 3.59 MeV which are not resolved in the present study. These four states were seen in the higher energy (d,^{2}He) study, and their analogs have been observed in the ^{24}Mg(p,n)^{24}Al reaction at excitation energies of 0.44, 1.07, 2.98, and 3.33 MeV, respectively. Their Gamow-Teller strengths from the (p,n) study, after adjusting for the isospin geometric factor (which is 1 in this case), are listed in Table I. The weak transition to the 0.47 MeV state has also been observed via β decay [31]. We note that the β-decay study gives a smaller value for the GT strength, B(GT) = 0.018, than that deduced from (p,n), B(GT) $\approx$ 0.05.

Figure 3 shows our measured 0° (d,^{2}He) cross sections at E_d=125.2 MeV as a function of the corresponding Gamow-Teller strengths deduced from β-decay studies, when available, or from (p,n) reactions. These values, as well as the corresponding nuclear structure information, are listed in Table I. Though the data are shown for nuclei in two different major shells, a remarkably well-defined linear relation is observed. Similar linear relations have been observed for (d,^{2}He) reactions at much higher energy, E_d=260 MeV [27], and in (p,n) studies [1]. This linear relation demonstrates that the (d,^{2}He) reaction at K500 cyclotron energies can also be used as a powerful tool to study Gamow-Teller strengths, in contrast to conclusions from earlier telescope studies at somewhat lower energies.

The solid line in Fig. 3 indicates a least-square fit of a linear relation, $\sigma=\alpha B$(GT), to the data. This fit yields a slope parameter, α=1.30±0.04 (mb/sr)/B(GT), with a χ^2 of

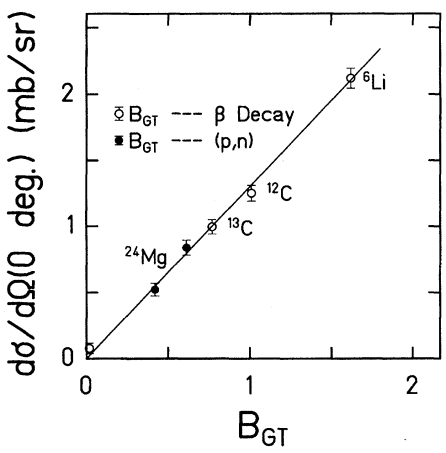

FIG. 3. The measured center-of-mass $(d,{}^2\mathrm{He})$ cross sections at 0° as a function of the Gamow-Teller strengths deduced either from β-decay studies or from (p,n) reactions. The solid line is a linear fit to the data. See the text for details.

3.8 for 5 degrees of freedom. Note that we use the $B(\mathrm{GT})$ value from the β-decay study for the transition to the 0.47 MeV state of ^{24}Na. A slightly better fit would be obtained by using the $B(\mathrm{GT})$ value from (p,n) study. The error bars in Fig. 3 include statistical errors, errors due to background subtraction, beam integration, and estimated errors due to ray-tracing efficiencies and detector acceptances from a Monte Carlo code. Uncertainties due to the assumption of S-wave breakup and the Watson-Migdal approximations [32] are not included. Overall, there could be a 30% or more uncertainty in the absolute normalization of the measured cross sections at this time. The relative error, as shown in Fig. 3, however, is much smaller. Moreover, the linear relation of the measured 0° cross sections with known Gamow-Teller strengths shown in Fig. 3 provides an empirical calibration of our detection system for our anticipated study of heavier nuclei which have important applications in double-beta-decay or nuclear astrophysics.

In conclusion, we have measured $(d,{}^2\mathrm{He})$ cross sections on ^{6}Li, ^{12}C, ^{13}C, and ^{24}Mg targets. The measured 0° cross sections show a well-defined linear relation with the known Gamow-Teller strengths deduced from β-decay and (p,n) studies. In contrast to negative conclusions from earlier studies [23–26] at somewhat lower energies, our results, extended to zero degrees, provide an unambiguously positive conclusion. The results clearly demonstrate that the $(d,{}^2\mathrm{He})$ reaction can be used to measure the Gamow-Teller strengths at energies as low as E_d=125.2 MeV.

We would like to acknowledge R. E. Tribble for many useful discussions during the course of this experiment. This work was supported in part by the U.S. DOE under Grant No. DE-FG03-93ER40773 and the Robert A. Welch Foundation.

[1] T.N. Taddeucci, C.A. Goulding, T.A. Carey, R.C. Byrd, C.D. Goodman, C. Gaarde, J. Larsen, D. Horen, J. Rapaport, and E. Sugarbaker, Nucl. Phys. **A469**, 125 (1987).

[2] C. Gaarde, J. Rapaport, T.N. Taddeucci, C.D. Goodman, C.C. Foster, D.E. Bainum, C.A. Goulding, M.B. Greenfield, D.J. Horen, and E. Sugarbaker, Nucl. Phys. **A369**, 258 (1981).

[3] F. Osterfeld, Rev. Mod. Phys. **64**, 491 (1992), and references therein.

[4] B.D. Anderson, T. Chittrakarn, A.R. Baldwin, C. Lebo, R. Madey, R.J. McCarthy, J.W. Watson, B.A. Brown, and C.C. Foster, Phys. Rev. C **31**, 1147 (1985); *ibid.* **31**, 1161 (1985).

[5] R. Madey, B. S. Flanders, B. D. Anderson, A. R. Baldwin, C. Lebo, J. W. Watson, S. M. Austin, A. Galonsky, B. H. Wildenthal, and C. C. Foster, Phys. Rev. C **35**, 2011 (1987).

[6] B. D. Anderson, N. Tamimi, A. R. Baldwin, M. Elaasar, R. Madey, D. M. Manley, M. Mostajabodda'vari, J. W. Watson, W. M. Zhang, and C. C. Foster, Phys. Rev. C **43**, 50 (1991).

[7] K. Ikeda, Prog. Theor. Phys. **31**, 434 (1964).

[8] B. A. Brown and B. H. Wildenthal, At. Data Nucl. Data Tables **33**, 347 (1985).

[9] N. Auerbach, G.F. Bertsch, B.A. Brown, and L. Zhao, Nucl. Phys. **A556**, 190 (1993).

[10] E. Caurier, A. P. Zuker, A. Poves, and G. Martinez-Pinedo, Phys. Rev. C **50**, 225 (1994).

[11] E. Caurier, A. Poves, and A. P. Zuker, Phys. Rev. Lett. **74**, 1517 (1995).

[12] C. Ellegard *et al.*, Phys. Rev. Lett. **59**, 974 (1987); Can. J. Phys. **65**, 600 (1987).

[13] See, e.g., M.B. Aufderheide, S.D. Bloom, D.A. Resler, and G.J. Mathews, Phys. Rev. C **48**, 1677 (1993); M.B. Aufderheide, I. Fushiki, S.E. Woosley, and D.H. Hartmann, Astrophys. J. Suppl. **91**, 389 (1994).

[14] W.P. Alford *et al.*, Nucl. Phys. **A514**, 49 (1990).

[15] F.P. Brady *et al.*, Phys. Rev. Lett. **48**, 860 (1982); Phys. Rev. C **43**, 2284 (1991).

[16] M.C. Vetterli *et al.*, Phys. Rev. Lett. **59**, 439 (1987); Phys. Rev. C **40**, 559 (1989).

[17] J. Rapaport *et al.*, Phys. Rev. C **41**, 1920 (1990).

[18] A. Ling *et al.*, Phys. Rev. C **44**, 2794 (1991).

[19] S. Yen, Can. J. Phys. **65**, 595 (1987).

[20] N. Anantaraman, J. S. Winfield, S. M. Austin, J. A. Carr, C. Djalali, A. Gillibert, W. Mittig, J. A. Nolan, Jr., and Z. W. Long, Phys. Rev. C **44**, 398 (1991).

[21] T. Ichihara *et al.*, Phys. Lett. B **323**, 278 (1994).

[22] H. Lenske, H. H. Wolter, and H. G. Bohlen, Phys. Rev. Lett. **62**, 1457 (1989).

[23] D. P. Stahel, R. Jahn, G. J. Wozniak, and J. Cerny, Phys. Rev. C **20**, 1680 (1979).

[24] K. B. Beard, J. Kasagi, E. Kashy, B. H. Wildenthal, D. L. Freisel, H. Nann, and R. E. Warner, Phys. Rev. C **26**, 720 (1982).

[25] T. Motobayashi, H. Sakai, N. Matsuoka, T. Saito, K. Hosono, A. Okihana, M. Ishihara, S. Shimoura, and A. Sakaguchi, Phys. Rev. C **34**, 2365 (1986).

[26] T. Motobayashi *et al.*, J. Phys. G **14**, L137 (1988).

[27] H. Ohnuma, Phys. Rev. C **47**, 648 (1993).

[28] T. Niizeki *et al.*, Nucl. Phys. **A577**, 37c (1994).

[29] A.C. Betker and C.A. Gagliardi, Nucl. Instrum. Methods **A283**, 76 (1989); A.C. Betker, Ph.D. dissertation, Texas A&M University (1993).

[30] A. C. Betker, R. H. Burch, and C. A. Gagliardi, Nucl. Instrum. Methods **A294**, 549 (1990).

[31] F. Ajzenberg-Selove, Nucl. Phys. **A490**, 1 (1988); **A506**, 1 (1990); **A523**, 1 (1991); P.M. Endt and C. van der Leun, *ibid.* **A521**, 1 (1990).

[32] K.M. Watson, Phys. Rev. **88**, 1163 (1952); A.B. Migdal, Zh. Eksp. Teor. Fiz. **28**, 3 (1955) [Sov. Phys. JETP **1**, 2 (1955)].